4th International Conference on Computational and Mathematical Biomedical Engineering – CMBE2015
29 June - 1 July 2015, France
P. Nithiarasu and E.Budyn (Eds.)

MORPHOMETRIC RETINAL MEASUREMENTS WITH ULTRA-WIDE-FIELD-OF-VIEW IMAGING

E Pellegrini[1], G Robertson[2], L Ballerini[1], T Pearson[2], T J MacGillivray[2] and E Trucco[1]
[1] VAMPIRE group, School of Computing, University of Dundee, DD1 4HN Dundee, UK
{e.z.pellegrini, l.ballerini, e.trucco}@dundee.ac.uk
[2] VAMPIRE group, Clinical Research Imaging Centre, University of Edinburgh, 47 Little France Crescent, Edinburgh, EH16 4TJ, UK {gavin.robertson, t.pearson, t.j.macgillivray}@ed.ac.uk

SUMMARY

Morphometric measurements of the retinal vasculature provide useful information for modelling. Much work exists on the location and quantitation of retinal vessels observed in fundus images, which capture a typical field of view within 50^o centered on the fovea or the optic disc. Much larger fields of view (beyond 200^o) can be captured with ultra-wide-field-of-view scanning laser ophthalmoscopes (UWFV SLO), enabling measurement of peripheral vessels without the need of mosaicking. We report here algorithms for vessel detection and analysis in UWFV SLO, developed in the framework of two studies on retinal biomarkers for cardiovascular disease and genetics.

Key words: *retinal image analysis, scanning laser ophthalmoscope, vessel detection, vessel measurement*

1 INTRODUCTION

Morphometric measurements of the retinal vasculature [1] provide useful information for modelling the retinal vasculature. Automatic techniques have been developed for locating blood vessels [7,8] and assessing their morphology, e.g., caliber, tortuosity and fractal dimension. Much of the existing work has concentrated on vessels observed in fundus images, which capture a typical field of view within 50^o centered on the fovea or the optic disc (henceforth OD). These remain the standard instruments encountered in clinics and opticians, but other instruments (e.g., OCT and its developments) are acquiring increasing importance for screening, diagnosis and quantitative assessment. One such instrument is *ultra-wide-field-of-view scanning laser ophthalmoscope* (UWFV SLO) [4], which allows non-mydriatic imaging of fields of view beyond 200^o horizontally. Large fields of view can achieved by mosaicking multiple fundus camera images, but this requires flashing light into the eye multiple times (done only once in UWFV SLO) and is therefore dependent on patient compliance in addition to mosaic quality.
UWFV SLO is a still under-researched modality in retinal image analysis [9,10]. We report here algorithms for vessel detection and assessment with UWFV SLO, developed in the framework of two studies on retinal biomarkers for cardiovascular disease and genetics. To our best knowledge, we are not aware of comparable algorithms for UWFV SLO.
In the first study, CARMEN (Cardiovascular Biomarkers from Wide-Field-of-View Retinal Scans) we have collected two prospective data sets of 500 patients each. The two groups were volunteers in two clinical trials, TASCFORCE [2] and SCOT-HEART [3]. TASCFORCE investigates the ability of a new screening program involving blood tests and MRI to identify people at increased risk of cardiovascular disease. SCOT-HEART is an outcome-focused prospective multicenter trial looking at the implementation of CT in the patient care pathway.
The second study relies on two cross-linked bioresources, ORCADES (www.orcades.ed.ac.uk/orcades) and GoDARTS (medicine.dundee.ac.uk/godarts) , which include fundus retinal images and genetic data (among others) available for biomarkers investigation. Here we studied the portability of algorithms developed for fundus images to UWFV SLO images.

2 METHODOLOGY

2.1. Modality comparison

We investigated the portability of vessel detection algorithms developed for fundus images to SLO images. We acquired a comparative data set of both eyes of 20 consented volunteers at the Ophthalmology Department of Ninewells NHS and University hospital, Dundee, first with a Topcon retinal camera (2336×3504 pixels), then with an OPTOS P200C SLO (3900×3072 pixels). We found significant differences in the accuracy of the location of the same vessels in the two modalities, mainly due to (a) different contrast, (b) different characteristics of central reflections in large vessels, and (c) the much larger field of view of UWFV SLO images, implying that the width of the same vessel in pixels can be half or less than in a fundus image. Leveraging these results, we developed the solution described in Section 2.2.

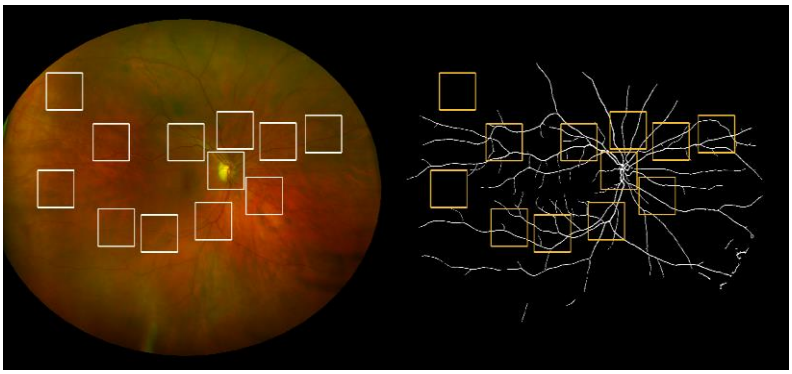

Figure 1. Left: example of UWFV SLO images with windows selected for tracing vasculature (ground truth generation). Right: binary map generated by the method sketched in Section 2.2.

2.2. Vessel detection

The vessel detection algorithm resulting from the comparative analysis of fundus and SLO images is based on neural networks. The key steps are as follows. An illumination correction step is performed, followed by image morphology with a structuring elements in 12 orientations, resulting in 12 maps. The pixelwise max-min difference is calculated to enhance the vessels. The difference image is convolved with 4 Laplacian of Gaussian filters to capture multiple spatial scales, each in 12 orientations as above. The maximum response is selected at each pixel over the orientations. The four LoG-filtered maps, the width map, and the standard deviations of direction maps form a feature vector which is input to a two-layer feed-forward network with sigmoid output neurons. The output of the network is a probability map of vessel pixel locations, finally processed by hysteresis thresholding.
Validation required ground truth annotations of the vasculature. As tracing the full vasculature in large OPTOS images is an extremely time-consuming task (~18 hours/image), we selected a representative sample (contrast, location, type of vessel, etc.) of 120 windows within which the vasculature was traced by 2 experts (Figure 1). Details have been reported elsewhere [5].

2.3. Vessel analysis

To estimate width, we first regularized the raw contours in the binary map with a parallel-constrained double spline [6], Figure 2 (c). We then estimated widths as the length of segments perpendicular to the double-spline centerline and contained within the vessel, Figure 2 (d).

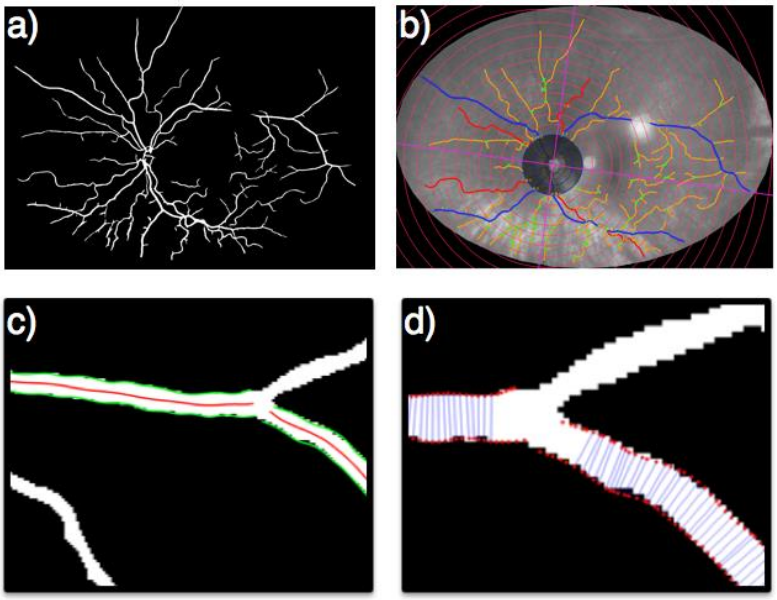

Figure 2. (a) Example of binary vessel map generated by the algorithm from an UWFV SLO image. (b) Vessel classification (not described) into veins (blue) and arteries (red), and unclassified (yellow). The red circles represent OD diameters from the OD centre. (c) Detail: parallel-constrained spline pair fitted to the vessel contours in the binary map to regularize the contours. (d) Detail: segments used for width estimation.

It has been observed that width estimation accuracy varies with width range, e.g. [8]. We divided vessels in 3 width range (small, medium, large), and achieved excellent accuracy against ground truth annotations of 144 widths on the set introduced in Section 2.2. Comparison against results obtained with adapted state-of-the-art algorithms (Soares, Bankhead, [8]) showed that our method achieved the best agreement with annotations. Full figures in final paper if accepted.

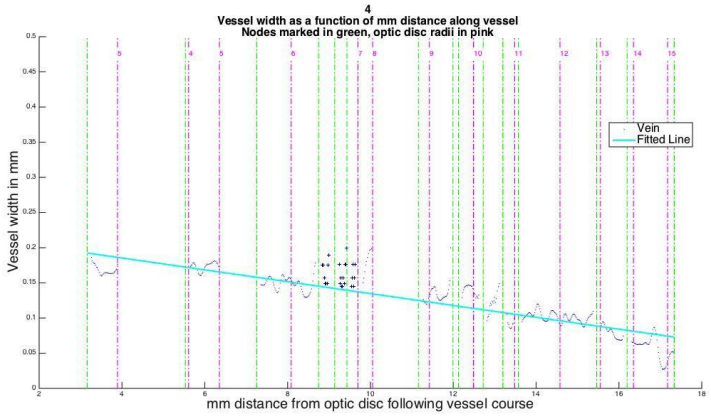

Figure 3. Width estimation for one of the main vessels in an UWFV SLO image, reaching out to 17 OD from the OD contour.

The availability of vasculature measurements over a much larger region than afforded by fundus cameras makes it possible to quantify larger portions of the vasculature, but also to explore biomarkers using novel retinal coefficients in addition to conventional calculations based on Zone B and C, i.e., up to 3 OD diameters from the OD contour; compare with Figure 2 (b). For instance, we can now compute the width of the main vessels with distance from the OD over 15 OD diameters from the OD contour, Figure 3.

2.5. GUI

All software packages enabling collection of retinal measurements used in clinical and screening centers are currently semi-automatic (e.g., SIVA, IVAN, CAIAR). Within VAMPIRE we have developed a GUI allowing efficient interaction, checking and correction of automatic results from

various modules (OD and fovea location, retinal co-ordinates, vasculature location, artery-vein classification, estimation of tortuosity, bifurcation angles, CRVE/CRAE, AVR, fractal dimension). This interface was adapted for the studies sketched here on UWFW images.

3 CONCLUSIONS

Our main findings can be summarized as follows. A comparative study looking at the same vessels imaged in different modalities suggests that vessel detection algorithms developed for fundus images cannot be ported directly to UWFV SLO images, given the different appearance of blood vessels in the two modalities mainly in terms of contrast and central reflection. Using images from the OPTOS P200C SLO, our validated vessel detection software solution achieved an accuracy of 0.965 and 0.967 AUC. Width can be calculated accurately even if vessels appear smaller than in fundus images (at a parity of resolution); we achieved excellent agreement with ground truth for small, medium and large vessels.
All studies mentioned, and the data access and acquisition they involved, were conducted in accordance to the standard ethical, safety and sponsorship rules in force in Scotland.

ACKNOWLEDGMENTS

L Ballerini was supported by Leverhulme Trust grant RPG-419 "Retinal Biomarkers for Large, Cross-Linked Genetic Data Sets". E Pellegrini and G Robertson were supported by SINAPSE/OPTOS grant "Cardiovascular Biomarkers from Wide-Field-of-View Retinal Scans" (CARMEN). We thank Jano van Hemert and Alan Fleming of OPTOS plc, and Dr Peter Wilson of Ninewells Ophthalmology, for invaluable input and support.

REFERENCES

[1] M. Abrámoff, M. Garvin, and M. Sonka. Retinal imaging and image analysis. IEEE Trans Med Imaging, 3:169-208, 2010.
[2] http://medicine.dundee.ac.uk/tascforce; http://www.isrctn.com/ISRCTN38976321
[3] D. E. Newby, M. C. Williams, A. D. Flapan et al. Role of multidetector computed tomography in the diagnosis and management of patients attending the rapid access chest pain clinic, The Scottish computed tomography of the heart (SCOT-HEART) trial: study protocol for randomized controlled trial. Trials, 13:184-188, 2012.
[4] R. H. Webb and G. W. Hughes. Scanning laser ophthalmoscope. IEEE Trans on Biomedical Engineering, 28:488-492, 1981.
[5] E. Pellegrini, G. Robertson, E. Trucco, T. J. MacGillivray, C. Lupascu, J. van Hemert, M. C. Williams, D. E. Newby, E. JR van Beek, and G. Houston, "Blood vessel segmentation and width estimation in ultra-wide field scanning laser ophthalmoscopy," Biomed. Opt. Express, 5:4329-4337, 2014.
[6] A. Cavinato, L. Ballerini, E. Trucco, and E. Grisan. Spline based refinement of vessel contours in fundus retinal images for width estimation. Proc IEEE EMBC, 2013, pp 872-87.
[7] M. M. Fraz, P. Remagnino, A. Hoppe, et al. Blood vessel segmentation methodologies in retinal images–a survey. Computer methods and programs in biomedicine, 108:407-433, 2012.
[8] C. A. Lupaşcu, D. Tegolo, and E. Trucco, "Accurate estimation of retinal vessel width using bagged decision trees and an extended multiresolution Hermite model," Med Image Anal 17, 1164–1180 (2013).
[9] M.S. Haleem, L. Han, J. van Hemert, et al. Retinal Area Detector from Scanning Laser Ophthalmoscope (SLO) Images for Diagnosing Retinal Diseases. IEEE Journ Biom and Health Informatics, volume PP, 2014.
[10] A. Rovira, R. Cabido, E. Trucco, et al. RERBEE: Robust Efficient Registration via Bifurcations and Elongated Elements applied to retinal fluorescein angiogram sequences. IEEE Trans Med Imaging, 31:140-150, 2012.